Journal of Mines, Metals and Fuels, *71(12C) : 41-48; 2023. DOI: 10.18311/jmmf/2023/47258*

Print ISSN : 0022-2755

Journal of Mines, Metals and Fuels

Contents available at: *www.informaticsjournals.com/index.php/jmmf*

Impact of Boundary Roughness and MHD on Saturation of Rayleigh-Taylor Instability at the Interface between Two Superposed Couple-Stress Fluids

Priya M. Gouder[1], G. B. Marali[2], Praveen I. Chandaragi[2*], Krishna B. Chavaraddi[3]

[1]Department of Mathematics, KLE Technological University, MSSCET, Belagavi Campus, Belagavi – 590008, Karnataka, India; priyagouder@klescet.ac.in

[2]Department of Mathematics, KLE Technological University, Hubballi – 580031, Karnataka, India; praveen.chandargi@kletech.ac.in, gbmarali@kletech.ac.in

[3]Department of Mathematics, S.S. Government First Grade College and P.G. Studies Center, Nargund – 582207, Karnataka, India; ckrishna2002@yahoo.com

Abstract

This study is about the influence at the boundary between two Couple-stress Casson fluids which are superposed on Rayleigh-Taylor instability (RTI) flowing in the existence of a uniform magnetic field acting normal to the surface in porous medium. The density of both the fluids is not the same. Established on fully developed approximations the stability analysis is applied, to achieve mathematical ease. The maximum wave numbers as well as resulting maximum frequency are found. In this analysis we discussed, the evolution of Rayleigh-Taylor unsteadiness due to non-Newtonian couple-stress Casson fluids over porous media. Graphical representations of stability that are discussed numerically based on the consequences of physical parameters for instance permeability parameter, non-Newtonian parameter, magnetic parameter, and couple-stress parameter.

Keywords: *Casson Fluid, Electro-Hydrodynamic Stability (EHD), Magnetic Field, Micro-Polar Fluid, Non-Newtonian Fluid, Porous Medium, Permeability, Viscosity*

1.0 Introduction

The "non-Newtonian fluid" pertains to a fluid, which deviates from Newton's law of viscosity. For non-Newtonian fluid the shear thinning behavior, is most prevalent in fluids where viscosity decreases under shear strain[1]. When studying fluid mechanics, it is important to understand how fluids flow through porous media and how they adhere to certain rules. Numerous areas of applied science and engineering make use of the concept of porous media[2]. When the denser fluid is accelerated by the lighter fluid, Chandrasekhar[3] deliberated the unsteadiness of a plane boundary amongst two incompressible viscous fluids having different densities. Investigation by Kent[4] on the stability analysis of parallel flows demonstrates significance of the horizontal magnetic field and draws the conclusion that it varies in the vertical direction. Also, revealed that under certain conditions the system is unstable, though the system is found to be stable in the non-existence of magnetic field. While the entire system is affected by a uniform magnetic field, Bhatia[5] supported by the impact of viscosity of a plane interface on stability analysis separated by two incompressible superposed conducting fluids possessing

**Author for correspondence*

uniform density. He analyzed stability pertaining to two extremely viscous liquids with same kinematic viscosity and dissimilar uniform densities. Sharma and Sharma[6] deliberated the work on the Rayleigh-Taylor unsteadiness amongst the two viscoelastic-superposed fluids.

The characteristics related to Casson fluid flow in a tube containing the standardized porous media is introduced by Dash[7] on the Rayleigh-Taylor unsteadiness a parameter related to Casson fluid flow through porous medium. This investigation is helpful in modeling the pathological condition concerned with flow of blood while cholesterol related to fatty plaques and the formation of artery obstruction blood clots in coronary artery lumen. He has considered the two cases related to permeability in case of porous medium. He analyzed consequence of permeability factor and on shear stress distribution produced stress of the liquid, plug flow radius, wall shear stress, and frictional resistance and flow rates.

Mohamed and Eldabe[8] investigated how an axial electric field affected a hollow jet's EHD stabilisation. The authors demonstrate the relationship between different system-related parameters and the electric field strength. By accounting for couette flow in the existence of an electric field applied normally, Eldabe[9] considered the electro-hydrodynamic steadiness of two stratified power law fluids. Eldabe[10] showed how the tangential electric field affects R-T instability. In the absence of gravity, Elhefnawy[11] examines the nonlinear evolution of electrohydrodynamic RTI at a cylindrical boundary that is separated by two conducting fluids with cross sections that are circular. The analysis above reflects a non-porous medium field.

Sunil[12] considered the Rayleigh-Taylor instability type, which is characterised by two Couple-stress fluids that are superposed possessing uniform densities operating in a porous medium with a uniform magnetic field applied horizontally. The investigation is focused on two highly viscous fluids with the same Couple-stress kinematic viscosity and kinematic viscosity. The author approximatedly determined the evolution rate of R-T instability. Rudraiah and Chandrashekara[13] discussed the consequence of couple-stress on the amount at which the R-T unsteadiness at the boundary evolves in a couple-stress liquid of finite thickness. In order to control R-T instabilities at the boundary between denser fluids that are accelerated by lighter ones, many recent works[14-17] demonstrates significance of couple stress fluid.

Agoor and Eldabe[18] took into account the RT instability at the boundary that develops in the porous medium due to the flow of superimposed couple-stress casson fluid and the importance of magnetic field. This project is a generalisation of Rudraiah and Chandrashekara's[13] work, which was concerned with flow of non-Newtonian fluid by a porous media in the existence of magnetic field applied externally. Additionally, the authors discussed impact of a normal magnetic field, permeability parameter, and couple stress on the unsteadiness of a type R-T casson fluid flow in a porous medium. The primary aim of the presemt work is to evaluate the analysis conducted by Agoor and Eldabe[18] using the no-slip condition at $y=0$.

This article is structured in the following order: The necessary basic equations, relevant boundary and surface conditions, in addition appropriate approximations are given in section 2. By using a linear stability study, the dispersion relation for two sets of boundary conditions is determined analytically in section 3. The findings and discussions are presented in section 4. The final section 5, provides the necessary conclusions.

2.0 Mathematical Formulation

In the physical configuration, two fluids have been taken into consideration, one of which is positioned on top of the other. The lower fluid is made up of a thin film with a composed thickness of $2a$ that is occupied by a non-Newtonian incompressible couple stress liquid with a constant density (p_1) of $1a$ and is enclosed by a rigid surface. The other non-Newtonian incompressible couple-stress liquid with constant density (p_2) (here $p_2 >> p_1$) and thickness d (here $d >> 2a$), is confining the film above; the boundary between the fluids is at $y=a$. As

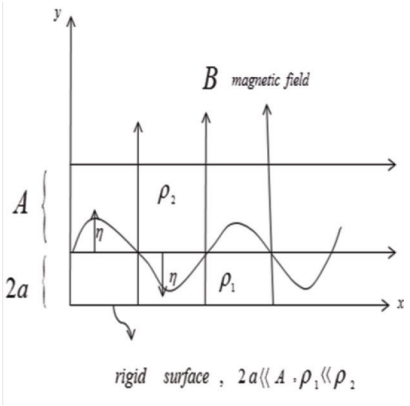


Figure 1.

revealed in Figure 1, the interface is applied a magnetic field of strength B that is subjected vertically along the *x*-axis (i.e. in positive *y*-direction).

For non-Newtonian incompressible couple stress fluid, the basic equations prevailing the motion along porous medium are specified by these equations in following form:

Continuity equation

$$\nabla.\vec{q}_1 = 0 \tag{2.1}$$

Equation of conservation of momentum is

$$\rho\left(\frac{\partial\vec{q}_1}{\partial t}+(\vec{q}_1.\nabla)\vec{q}_1\right)= -\nabla p+\mu\nabla^2\vec{q}_1+\nabla.\tau+\frac{\mu}{k^*}\vec{q}_1+(\vec{J}\times\vec{B})-\lambda^*\nabla^4\vec{q}_1 \tag{2.2}$$

Here

$$\vec{J}=\sigma\left(\vec{E}+\vec{q}_1\Lambda\vec{B}\right)+\rho_e\vec{q}_1,\quad \vec{B}=\vec{B}j,\quad \vec{q}_1=\left(u(y),v,0\right) \tag{2.3}$$

$\tau\left(\tau_{ij}\right)$ represents stress tensor involving bi-viscosity Casson effect[19]. Bi-viscosity model represents constitutive equation related to blood, which is given by following form:

$$\tau_{ij}=\begin{cases}2\left(\mu_B+\frac{p_y}{\sqrt{2\pi}}\right)e_{ij}, & \pi\geq\pi_c\\ 2\left(\mu_B+\frac{p_y}{\sqrt{2\pi_c}}\right)e_{ij}, & \pi\leq\pi_c\end{cases} \tag{2.4}$$

here $\pi=\left(e_{ij}e_{ji}\right)$ and e_{ij} is $(i,j)^{th}$ components of rate of deformation specified as

$$e_{ij}=\frac{1}{2}\left(\frac{\partial q_i}{\partial x_i}+\frac{\partial q_j}{\partial x_j}\right) \tag{2.5}$$

Conferring to the interpretation assumptions in Rudraiah and Chandrashekara[13], let us suppose that S (measure of local acceleration to inertial acceleration, the Strouhal number) is $S=\frac{L^*}{UT}\ll 1$. where $U=\frac{v}{L^*}$, $v=\frac{\mu}{\rho}$, $L^*=\sqrt{\frac{\gamma}{\xi}}$ is characteristic length, $\delta=g(\rho_1-\rho_2)$, and $T=\frac{\mu\gamma}{a^3\delta^2}$. We can ignore the local acceleration term $\frac{\partial u}{\partial t}$ according to S << 1, also we can take $\frac{\partial v}{\partial t}=0$. The inertial acceleration term $v\frac{\partial u}{\partial y}$ is negligible in comparison with high viscous couple stress fluid. The interface elevation, η is supposed to be insignificant in comparison with 2a, the film thickness i.e., $\frac{\eta}{a}\ll 1$.

The preceding suppositions enable to employ the creeping flow approximation that further enables to ignore some specific terms arising in the perturbation equation to find linear equations resulting from interface elevation. Applying Eqs. (2.3) and (2.5) and the aforementioned assumptions, Eqs. (2.1) and (2.2) reduce to

$$\frac{\partial u}{\partial x}+\frac{\partial v}{\partial y}=0 \tag{2.6}$$

$$0=-\frac{\partial p}{\partial x}+\left(\mu+\mu_B\right)\frac{\partial^2 u}{\partial y^2}-\frac{\mu}{k^*}u-\sigma B^2u-\lambda^*\frac{\partial^4 u}{\partial y^4} \tag{2.7}$$

$$0=-\frac{\partial p}{\partial y}-\frac{\mu}{k^*}v \tag{2.8}$$

For analyzing the problem under consideration, the suitable boundary and surface conditions are applied. In accordance with Rudraiah and Chandrashekara[13] the conditions pertaining to boundary, suitable for the problem under study at the rigid surface is the no-slip condition:

$$u,v=0\quad at\ y=0 \tag{2.9}$$

$$\frac{\partial u}{\partial y}=0\ at\ y=a \tag{2.10}$$

$$\frac{\partial^2 u}{\partial y^2}=0\ at\ y=\pm a \tag{2.11}$$

$$p=-\delta\eta-\gamma\frac{\partial^2\eta}{\partial x^2}\ at\ y=a \tag{2.12}$$

$$v=\frac{\partial\eta}{\partial t}+u\frac{\partial\eta}{\partial x}\quad at\quad y=a \tag{2.13a}$$

In case of linearity, Eq. (2.13a) becomes

$$v=\frac{\partial\eta}{\partial t}\quad at\quad y=a \tag{2.13}$$

Let us non- dimensionalized the variables using the following substitution

$$v=\frac{\delta a^2}{\mu}v',u=\frac{\delta a^2}{\mu}u',p=\delta ap',$$
$$\eta=a\eta',t=\frac{\mu}{\delta a}t',x=ax',y=ay',$$
$$M=\frac{\sigma B^2a^2}{\mu},k=a^2k',\lambda=\mu a^2\lambda',\alpha=\frac{\mu_B}{\mu}. \quad (2.14)$$

Eq. (2.7) and Eq. (2.8) in non-dimensonalized form reduces to:

$$\lambda D^4u-(1+\alpha)D^2u+\left(M+\frac{1}{k}\right)u=-\frac{\partial p}{\partial x} \quad (2.15)$$

$$\text{and } -\frac{\partial p}{\partial y}=\frac{1}{k}v \quad (2.16)$$

Applying the boundary conditions:

$$\left.\begin{aligned} u,v&=0 \quad at\ \ y=0\\ \frac{\partial u}{\partial y}&=0\ \ at\ \ y=1\\ \frac{\partial^2u}{\partial y^2}&=0\ at\ y=\pm1\\ p&=-\delta\eta-\frac{1}{\beta}\frac{\partial^2\eta}{\partial x^2}\ at\ \ y=1\\ v&=\frac{\partial\eta}{\partial t}\quad at\ \ y=1 \end{aligned}\right\} \quad (2.17)$$

here $\beta=\frac{\delta a^2}{\gamma}$. Solution of Eq. (2.15) and Eq. (2.16), by using the boundary conditions indicated in Eq. (2.17) is:

$$u(y)=-\left(\frac{k}{kM+1}\right)\frac{\partial p}{\partial x}+C_1e^{Ay}+C_2e^{-Ay}+C_3e^{by}+C_4e^{-by} \quad (2.18)$$

where

$$C_1=\frac{\left(\frac{k}{kM+1}\right)\frac{\partial p}{\partial x}\Delta_1}{\Delta},\ C_2=\frac{\left(\frac{-k}{kM+1}\right)\frac{\partial p}{\partial x}\Delta_2}{\Delta},$$
$$C_3=\frac{\left(\frac{k}{kM+1}\right)\frac{\partial p}{\partial x}\Delta_3}{\Delta},C_4=\frac{\left(\frac{-k}{kM+1}\right)\frac{\partial p}{\partial x}\Delta_4}{\Delta}.$$

$$\Delta_1=\begin{vmatrix} -Ae^{-A} & be^{b} & -be^{-b}\\ A^2e^{-A} & b^2e^{b} & b^2e^{-b}\\ A^2e^{A} & b^2e^{-b} & b^2e^{b}\end{vmatrix},$$

$$\Delta_2=\begin{vmatrix} Ae^{A} & be^{b} & -be^{-b}\\ A^2e^{A} & b^2e^{b} & b^2e^{-b}\\ A^2e^{-A} & b^2e^{-b} & b^2e^{b}\end{vmatrix},$$

$$\Delta_3=\begin{vmatrix} Ae^{A} & -Ae^{-A} & -be^{-b}\\ A^2e^{A} & A^2e^{-A} & b^2e^{-b}\\ A^2e^{-A} & A^2e^{A} & b^2e^{b}\end{vmatrix},$$

$$\Delta_4=\begin{vmatrix} Ae^{A} & -Ae^{-A} & be^{b}\\ A^2e^{A} & A^2e^{-A} & b^2e^{b}\\ A^2e^{-A} & A^2e^{A} & b^2e^{-b}\end{vmatrix}$$

$$\Delta=\begin{vmatrix} 1 & 1 & 1 & 1\\ Ae^{A} & -Ae^{-A} & be^{b} & -be^{-b}\\ A^2e^{A} & A^2e^{-A} & b^2e^{b} & b^2e^{-b}\\ A^2e^{-A} & A^2e^{A} & b^2e^{-b} & b^2e^{b}\end{vmatrix}.$$

$$A=\frac{1}{\sqrt{2}}\sqrt{\left\{\frac{(1+\alpha)}{\lambda}+\frac{\sqrt{\left[(k+k\alpha)^2+4k\lambda(kM+1)\right]}}{k\lambda}\right\}},$$
$$b=\frac{1}{\sqrt{2}}\sqrt{\left\{\frac{(1+\alpha)}{\lambda}-\frac{\sqrt{\left[(k+k\alpha)^2+4k\lambda(kM+1)\right]}}{k\lambda}\right\}}. \quad (2.19)$$

By using Eq. (2.18) and Eq. (2.19), we get:

$$u(y)=\left(\frac{k}{kM+1}\right)\frac{\partial p}{\partial x}\left\{\begin{matrix}-1+\frac{\Delta_1}{\Delta}e^{Ay}-\frac{\Delta_2}{\Delta}e^{-Ay}\\ +\frac{\Delta_3}{\Delta}e^{by}-\frac{\Delta_4}{\Delta}e^{-by}\end{matrix}\right\} \quad (2.20)$$

3.0 Dispersion Relation

Rudraiah and Chandrashekara[13] asserts that by integrating with respect to y between the limits *y=-1* and *y=1* in order to solve the continuity equation (2.16a), we obtain:

$$v(1)=\left(\frac{-2k}{kM+1}\right)\frac{\partial^2p}{\partial x^2}\left\{\begin{matrix}-1+\left(\frac{\Delta_1-\Delta_2}{A\Delta}\right)\sinh A\\ +\left(\frac{\Delta_3-\Delta_4}{b\Delta}\right)\sinh b\end{matrix}\right\} \quad (2.21)$$

By substituting in Eq. (2.21) with the boundary conditions Eq.(2.17) and letting $\eta = \eta_0 e^{-ilx+nt}$, the following dispersion relation is obtained.

$$n = \left(\frac{2kl^2}{kM+1}\right)\left(1-\frac{l^2}{\beta}\right)\left\{\begin{matrix} 1-\left(\frac{\Delta_1-\Delta_2}{A\Delta}\right)\sinh A \\ -\left(\frac{\Delta_3-\Delta_4}{b\Delta}\right)\sinh b \end{matrix}\right\} \tag{2.22}$$

here l is wave number, n is frequency, and M is magnetic parameter, and signifies the evolution frequency of the interface as a function of the couple stress parameter (λ), the non-Newtonian parameter (α), the permeability of the porous media (k), and the magnetic parameter (M). The growth rate given by Eq. (2.22) assumes the following shape in the nonexistence of the couple stress parameter (λ):

$$n_b = \left(\frac{2kl^2}{kM+1}\right)\left(1-\frac{l^2}{\beta}\right) \tag{2.23}$$

This only depends upon the magnetic parameter *(M)*, the porous medium's permeability (k), the wave number (l) and the Bond number (β), being the surface tension's precise reciprocal.

4.0 Results and Discussion

By applying the normal mode analysis, the analytical result is discovered in the proposed investigation. When the critical cut-off wave number is equated to zero using the dispersion relation represented by Eq. (2.22), the effect is as shown in the following Eq (2.24).

$$l_{ct} = \sqrt{\beta} \tag{2.24}$$

However, at $\frac{\partial n}{\partial l} = 0$, the maximum wave number can be written as

$$l_{\max} = \frac{l_{ct}}{\sqrt{2}} \tag{2.25}$$

The maximum growth rate can be obtained in the form as

$$n_{\max} = \left(\frac{-k\beta}{2(kM+1)}\right)\left\{\begin{matrix} 1-\left(\frac{\Delta_1+\Delta_2}{A\Delta}\right) \\ \sinh A-\left(\frac{\Delta_3+\Delta_4}{b\Delta}\right)\sinh b \end{matrix}\right\} \tag{2.26}$$

$$n_{b\ \max} = \frac{k\beta}{2(kM+1)} \tag{2.27}$$

Using Eqs. (26) and (27), the G_{max}, representing ratio of the growth rates can be found as:

$$G_{\max} = \frac{n_{\max}}{n_{b\ \max}} = \left\{\begin{matrix} 1-\left(\frac{\Delta_1-\Delta_2}{A\Delta}\right)\sinh A \\ -\left(\frac{\Delta_3-\Delta_4}{b\Delta}\right)\sinh b \end{matrix}\right\} \tag{2.28}$$

A sequence of Figures illustrates how the magnetic parameter M, couple stress parameter λ, non-Newtonian parameter α, permeability parameter k, and bond number β affect the evolution rate n (frequency). The relationship between the frequency parameter n and the couple-stress parameter, λ is depicted in Figure 2. It should be noted that as the value of λ rises, the value of n falls. The dependency of n on the magnetic parameter M is shown in Figure 3. It is observed that growth rate significantly decreases as the value of M rises from 0 to 2.5, indicating that stability in the existence of magnetic field can be attained by significantly reducing magnetic field intensity. Figure 4 shows the behaviour of the permeability parameter k. We can infer from Figure 4 that the frequency value n rises as the value of permeability parameter k increases. The influence of the Bond number, β on the growth rate n is revealed in Figure 5. With a gradual increase in the Bond number from 2 to 10, the evolution rate n rises. As seen in Figure 6, a reduction in the value of n results from an increase in the value of non-Newtonian (Casson fluid) parameter α. The consequence of the porosity parameter, σ_p on the stability analysis is shown in Figure 7. The value of n decreases from 4 to 20 as the porosity parameter σ_p value increases.

5.0 Conclusion

Theoretically, a magnetic field-induced flow of Casson fluid through a porous media with couple stress fluids is examined for the Rayleigh-Taylor instability. In order to model this study mathematically, a set of differential equations is used. When boundary and surface conditions are suitable, fluid flow is what regulates the system. Under some appropriate approximations and assumptions, the system of equations is considered to find the dispersion relation. The stability region is taken

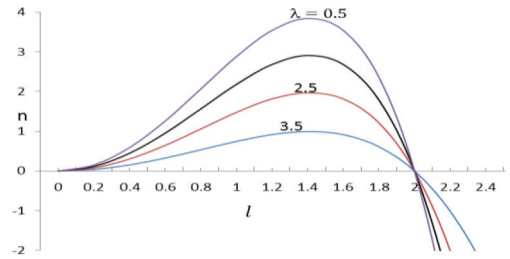


Figure 2. Evolution rate n for various values of couple stress parameter l with fixed values as $\alpha_p = 0.1, \beta = 4, \alpha = 5,\ k = 2.5, \sigma_p = 4, M = 2.$

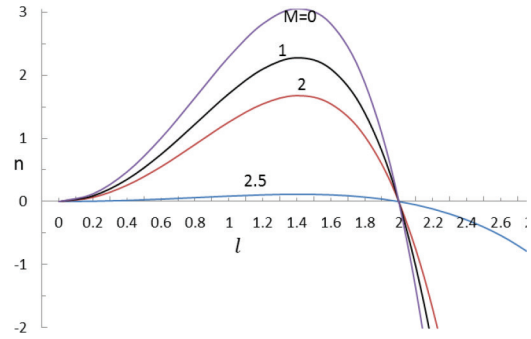


Figure 3. Evolution rate n for different values of magentic intensity M with fixed values $\alpha_p = 0.1, \beta = 4, \alpha = 5, k = 2.5, \sigma_p = 4, \lambda = 3.$

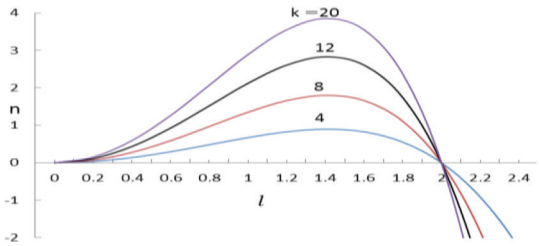


Figure 4. Evolution rate n for different values of permeability parameter k with fixed values $\alpha_p = 0.1, \beta = 4, \alpha = 5,\ \sigma_p = 4, \lambda = 3, M = 2.$

into account numerically in relation to a number of physical parameters related to the problem, for instance the couple stress parameter λ, the magnetic parameter M, the non-Newtonian parameter α, the permeability parameter k and the bond number β. The significance of these is illustrated visually in a series of figures. The Bond number β and the permeability parameter, together with their combined effects, have been found to

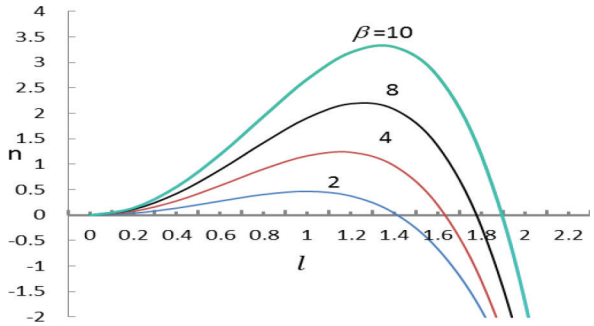


Figure 5. Evolution rate n for different values of bond number b with fixed values $\alpha_p = 0.1, \alpha = 5, k = 2.5, \sigma_p = 4, \lambda = 3, M = 2.$

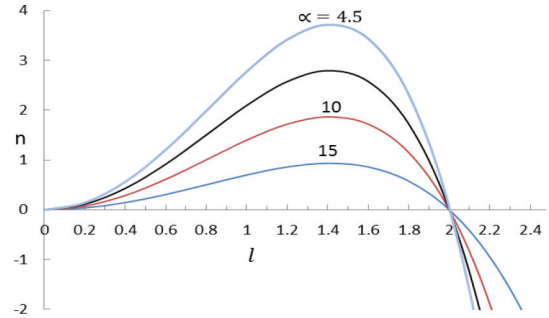


Figure 6. Evolution rate n for different values of Casson fluid parameter α with fixed values $\alpha_p = 0.1, \beta = 4, k = 2.5,\ \sigma_p = 4, \lambda = 3, M = 2.$

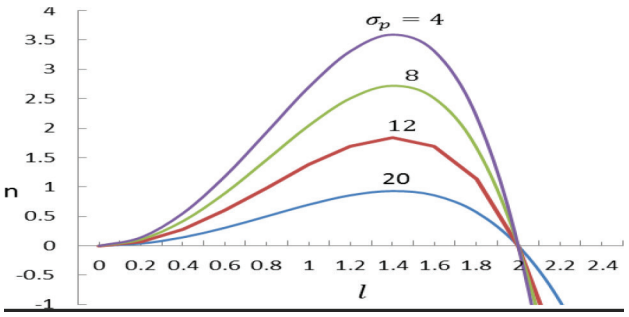


Figure 7. Evolution rate n for different values of Porosity parameter σ_p with fixed values $\alpha_p = 0.1, \beta = 4, \alpha = 5, k = 2.5, \lambda = 3, M = 2.$

attain stability of the boundary between the two fluids. The couple stress parameter, magnetic parameter M, non-Newtonian parameter, α and porosity parameter σ_p however, exhibits destabilization the growth rate of the system.

6.0 References

1. Mezger TG. The rheology handbook: For users of rotational and oscillatory rheometers, Rev. Ed. Hannover: Vincentz Network; 2006.
2. Zheng X, Shen G, Wang C, Li Y, Dunphy D, Hasan T, *et al.* Bio-inspired Murray materials for mass transfer and activity. Nat Commun. 2017; 8:14921. https://doi.org/10.1038/ncomms14921
3. Chandrasekhar S. Hydrodynamic and hydro magnetic stability, New York: Dover Publication; 1981.
4. Kent A. Instability of laminar flow of a perfect magneto-fluid. Phys Fluids. 1966; 9:1286-9. https://doi.org/10.1063/1.1761842
5. Bhatia PK. Rayleigh-Taylor instability of two viscous superposed conducting fluids. Il Nuovo Cimento B (1971-1996). 1974; 19:161-8. https://doi.org/10.1007/BF02895637
6. Sharma RC, Sharma KC. Rayleigh Taylor instability of two superposed conducting fluids in presence of suspended particles. Acta Phys Acad Sci Hung. 1978; 45:213-40. https://doi.org/10.1007/BF03157252
7. Dash RK, Mehta KN. Casson fluid flow in a pipe fluid with a homogeneous porous medium. Int. J Eng Sci. 1996; 34(10):1145-56. https://doi.org/10.1016/0020-7225(96)00012-2
8. Mohamed AEMA, ElDabe NT. Electrohydrodynamic stability a hollow jet. J Mathemat Phys Soc Egypt. 1978; 45.
9. ElDabe NT. Electro hydrodynamic stability of two superposed elastico-viscous liquids in plane coutte flow. J Math Phys. 1988; 29(1):2790-800.
10. ElDabe NT. Effect of a tangential electric field on Rayleigh-Taylor instability. Journal of the Physical Society of Japan. 1989; 58(1):115-20. https://doi.org/10.1143/JPSJ.58.115
11. Bothaina ARFE, Agoor MH, Elcoot AEK. Nonlinear electrohydrodynamic stability of a finitely conducting jet under an axial electric field. Physica A Stat Mech Appl. 2001; 297(3-4):368-88.
12. Sunil, RCS, Chandel RS. On superposed couple-stress fluids in porous medium in hydro magnetics. Z fur Naturforsch. 2002; 57(12):955-60. https://doi.org/10.1515/zna-2002-1208
13. Rudraiah N, Chandrashekara G. Effects of couple-stress on the growth rate of Rayleigh-Taylor instability at the interface in a finite thickness couple-stress fluid. J Appl Fluid Mech. 2010; 3(1):83-9. https://doi.org/10.36884/jafm.3.01.11882
14. Gouder PM, Chandaragi PI, Chavaraddi KB, Marali GB. Influence of boundary roughness on magnetohdyridynamic KH instability in couple-stress fluids. J Adv Res Fluid Mech Therm Sci. 2021; 88(2):93-105. https://doi.org/10.37934/arfmts.88.2.93105
15. Chavaraddi KB, Nandeppanavar MN, Awati VB, Gouder PM. The effect of the magnetic field on the Rayleigh-Taylor instability in a couple-stress fluid. Int J Appl Mech Eng. 2018; 23(3):611-22. https://doi.org/10.2478/ijame-2018-0033
16. Chavaraddi KB, Gouder PM, Kudenatti RB. The influence of boundary roughness on Rayleigh-Taylor instability at the interface of superposed couple-stress fluids. J Adv Res in Fluid Mech Thermal Sci. 2020; 75(2): 1-10. https://doi.org/10.37934/arfmts.75.2.110
17. Awati VB, Chavaraddi KB, Gouder PM. Effect of boundary roughness on nonlinear saturation of Rayleigh-Taylor instability in couple-stress fluid. Nonlinear Eng. 2019; 8(1):39-45. https://doi.org/10.1515/nleng-2018-0031
18. Agoor BM, Eldabe NTM. RTI at the interface of superposed couplestress Casson fluids flow in porous medium under the effect of magnetic field. J Appl Fluid Mechanics. 2014; 7(4):573-80.
19. Nakamura M, Sawada T. Numerical study on the flow of a non-Newtonian fluid through an axis symmetric stenosis, ASME J Biomech Eng. 1988; 110(2):137-43. https://doi.org/10.1115/1.3108418

NOMENCLATURE

G_{max}	ratio of growth rate	a	non-Newtonian Parameter.
G	gravitational acceleration		
K	permeability parameter	γ	Surface tension
L	wave number	n	elevation of the interface
M	magnetic parameter	λ	couple stress parameter
N	frequency (growth rate)	u_{β}	plastic dynamic viscosity
P	Pressure	u	coefficient of viscosity
p_y	yield stress	v	kinematic viscosity
Qi	Velocity	p	density of the fluid
T	characteristic time scale	T_{ij}	stress tensor
β	bond number	U	characteristic velocity